Journal of Organometallic Chemistry, 472 (1994) 247–255

Synthesis and electronic structure of rigid rod octahedral Ru-σ-acetylide complexes *

Muhammad S. Khan, Ashok K. Kakkar, Scott L. Ingham, Paul R. Raithby and Jack Lewis
University Chemical Laboratory, Lensfield Road, Cambridge CB2 1EW (UK)

Brock Spencer
Department of Chemistry, Beloit College, Beloit, WI (USA)

Felix Wittmann and Richard H. Friend
Cavendish Laboratory, Madingley Road, Cambridge CB3 0HE (UK)

(Received September 16, 1993)

Abstract

Syntheses of the mono-, bis- and poly-nuclear Ru-σ-acetylide complexes, *trans*-$[Ru(CO)_2(P^nBu_3)_2(-C{\equiv}C-C_6H_5)_2]$, *trans*-$[ClRu(CO)_2(P^nBu_3)_2-C{\equiv}C-p-C_6H_4-C_6H_4-p-C{\equiv}C-Ru(CO)_2(P^nBu_3)_2Cl]$ and *trans*-$[-Ru(CO)_2(P^nBu_3)_2-C{\equiv}C-R-C{\equiv}C-]_n$ (R = $p-C_6H_4$, $p-(CH_3)_2C_6H_2$) are reported. A study of the electronic structure of model metal–acetylide complexes of Group 8, $M(L)_2(L')_2(RH)_2$, $ClRu(L \text{ or } L')_4-R-Ru(L \text{ or } L')_4Cl$, $[M(PH_3)_4(RH)]_2R$ and $[M(L)(L)_2(R)]_n$ (M = Fe, Ru; L = L' = PH_3, PMe_3; L = CO, L' = PH_3; R = $-C{\equiv}C-$, $-C{\equiv}C-C_6H_4-C{\equiv}C-$, $-CH{=}CH-p-C_6H_4-CH{=}CH-$) has been carried out using the Fenske-Hall molecular orbital model. These results and a comparison of the IR ($\nu_{C{\equiv}C}$ stretching frequencies) and optical absorption ($\pi-\pi^*$ energy band gap) spectra of these complexes provide evidence for the role of (i) auxiliary ligands, (ii) metal, and (iii) the bridging alkyne units in determining the extent of π-electron conjugation in the backbone of these rigid rod organometallic complexes.

Key words: Ruthenium; Electronic structure; Molecular orbital calculations; Polymer; Acetylene; Phosphine

1. Introduction

Extended one-dimensional π-electron delocalization in a macromolecule imparts intriguing physical and chemical properties with potential technological applications [1]. Conjugated organometallic polymers, $[-M(L)_nC{\equiv}C-R-C{\equiv}C-]_n$, containing transition metal centers linked *via* organic moieties [2] offer promise for properties such as third-order non-linear optical effects [3] and liquid crystalline behavior [4]. A detailed understanding of structure-property relationships in these complexes is essential to exploit the chemical design of new materials fully. Our approach to gain insight in this area has been to study the factors that contribute to the extent of π-electron delocalization in the backbone by varying the metal, the auxiliary ligands and the connecting organic moieties. We report herein synthesis and characterization of monomeric, *trans*-$[Ru(CO)_2(P^nBu_3)_2(-C{\equiv}C-C_6H_5)_2]$ and the first examples of a soluble dimeric complex, *viz.* $[ClRu(CO)_2(P^nBu_3)_2-C{\equiv}C-p-C_6H_4-C_6H_4-C{\equiv}C-Ru(P^nBu_3)_2(CO)_2Cl]$, and for polymeric complexes, viz. $[-Ru(CO)_2(P^nBu_3)_2-C{\equiv}C-R-C{\equiv}C-]_n$ (R = $p-C_6H_4$, $p-(CH_3)_2C_6H_2$), and the results of a detailed study of the electronic structure of the model Group 8 metal-σ-acetylide complexes, $M(L)_2(L')_2(RH)_2$, $ClRu(L \text{ or } L')_4-R-Ru(L \text{ or } L')_4Cl$, $[M(PH_3)_4(RH)]_2R$ and $[M(L)_2(L')_2(R)]_n$ (M = Fe, Ru; L = L' = PH_3, PMe_3; L = CO, L' = PH_3; R = $-C{\equiv}C-$, $-C{\equiv}C-C_6H_4-C{\equiv}C-$,

Correspondence to: Professor the Lord Lewis or Dr. B. Spencer or Dr. R.H. Friend.

* Dedicated to Prof. Dr. Helmut Werner on the occasion of his 60th birthday.

0022-328X/94/$7.00
SSDI 0022-328X(93)24258-7

$-CH{=}CH-C_6H_4-CH{=}CH-$). The calculations provide a useful overview of the effects of tuning the properties of such polymers by substitution of ancillary ligands at the metal center, changing the metal, and altering the nature of the conjugated backbone alkyne ligand. The results are supported by a comparison of the IR $\nu_{C\equiv C}$ stretching frequencies, and the electronic absorption spectra of the title complexes.

2. Results and discussion

2.1. Synthesis

The synthetic strategy (Scheme 1) is based on a Me_3Sn-alkynyl ligand exchange route developed recently for a series of transition metal σ-acetylide complexes [5]. The monomeric Ru-bis-acetylide complex $[Ru(CO)_2(P^nBu_3)_2(-C{\equiv}C-C_6H_5)_2]$ (**3**) was prepared by reaction of $Ru(CO)_2(P^nBu_3)_2Cl_2$ (**1**) with 2.5 equivalents of $Me_3Sn-C{\equiv}C-C_6H_5$ (**2**) in THF in the presence of a catalytic amount of CuI. A series of similar Ru-bis-acetylide complexes, *trans*-$[Ru(CO)_2(PEt_3)_2-C{\equiv}C-R)_2]$ (R = H, C_6H_5, ^{t}Bu, $SiMe_3$) was prepared recently from $Ru(CO)_2(PEt_3)_2Cl_2$ and the corresponding Li-alkynyl reagents by Sun *et al.* [6]. A rigid rod-type *trans* arrangement of the acetylenic units around Ru in such Ru-bisacetylide complexes was confirmed by single crystal X-ray diffraction study of *trans*-$[Ru(CO)_2(PEt_3)_2(-C{\equiv}C-R)_2]$ (R = H, C_6H_5) [6] and *trans*-$[Ru(DPPE)_2(-C{\equiv}C-C_6H_5)_2]$, [7] where DPPE = 1,2-bis(diphenylphosphinoethane).

Treatment of 2.2 equivalents of (**1**) with one equivalent of $Me_3Sn-C{\equiv}C-p-C_6H_4-C_6H_4-p-C{\equiv}C-SnMe_3$ (**4**) in tetrahydrofuran yields the bimetallic complex, $[Cl-Ru(CO)_2(P^nBu_3)_2-C{\equiv}C-p-C_6H_4-C_6H_4-p-C{\equiv}C-Ru(P^nBu_3)_2(CO)_2Cl]$ (**5**). When a similar reaction is carried out with an equimolar mixture of (**1**) and (**6** or **7**) in the presence of a catalytic amount of CuI, the polymeric complexes $[-Ru(CO)_2(P^nBu_3)_2-C{\equiv}C-R-C{\equiv}C-]_n$ (R = $p-C_6H_4$ (**8**), $p-C_6H_2(CH_3)_2$ (**9**)) are obtained. These complexes (**5**, **8**, **9**) are soluble in common organic solvents, and were purified by column chromatography on alumina with dichloromethane as eluant. The molecular weights of the polymeric complexes (**8**, **9**) were determined by gel permeation chromatography [8].

2.2. Spectroscopy

Metal-to-alkyne ligand charge transfer (MLCT) is a common spectral feature of the transition metal σ-acetylide complexes, and reflects the extent of π-electron conjugation in these complexes. With an increase in π-conjugation, strong shifts in the optical absorption

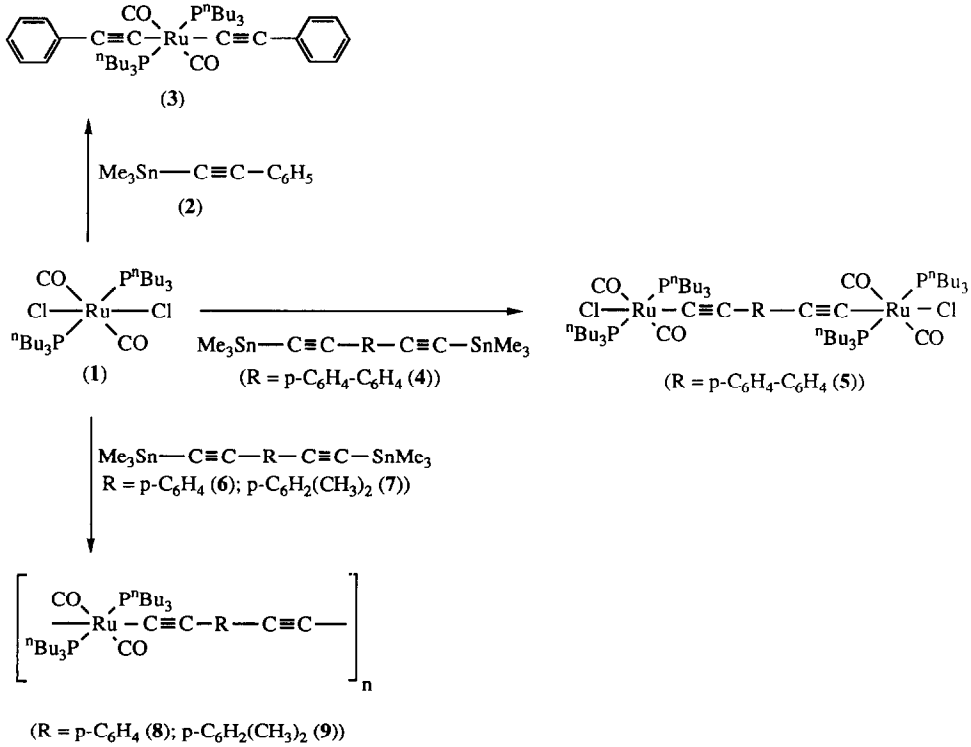

Scheme 1.

[9] and $\nu_{C\equiv C}$ infrared transition to lower energies are observed. The solubility of the Ru-σ-acetylide complexes (especially of the polymeric complexes) in dichloromethane allows an evaluation of their optical properties. The results of the optical absorption measurements are summarised in Table 1. The complexes show strong absorptions, which are assigned to MLCT transitions. The optical absorption spectra of the complexes provide minimum excitation energy values which indicate that the band gap (Table 1) is lower for the polymeric complexes (**8**, **9**) than for the bimetallic complex (**5**) by 0.90 eV. This is in agreement with the previous results on platinum σ-acetylide complexes [9], and shows that the π-electron conjugation is maintained through the Ru^{2+} centers in these complexes. The band gaps for the polymeric complexes containing mixed auxiliary ligands, $[-Ru(CO)_2(P^nBu_3)_2-C\equiv C-R-C\equiv C-]_n$ (approximately 3.5 eV) are much higher than for the analogous complexes containing only phosphine ligands, $[-Ru(DEPE)_2-C\equiv C-R-C\equiv C-]_n$ (3.07–3.25 eV). Also the minimum excitation energies for the Ru^{2+} dimer (**5**, 4.4 eV) and the polymeric complexes (**8**, **9** approximately 3.5 eV) containing the mixed auxiliary ligands are higher than for the corresponding Pt^{2+} complexes containing only phosphine ligands (bimetallic complex, 3.60 eV; polymeric complex, 3.26 eV) [9] (Table 1).

The IR spectra of the Ru-σ-acetylide complexes show a single strong $\nu_{C\equiv C}$ absorption consistent with *trans*-configuration of the acetylenic units around Ru. Several important features are evident from the IR data presented in Table 1:

(i) the $\nu_{C\equiv C}$-stretching frequency for the polymeric complexes, $[-Ru(CO)_2(P^nBu_3)_2-C\equiv C-R-C\equiv C-]_n$ (2085 cm^{-1}) (**8**, **9**) is 21 wave numbers lower than for the bimetallic complexes (**5**) (2106 cm^{-1}), indicating a higher degree of conjugation in the former;

(ii) the $\nu_{C\equiv C}$-stretching frequency is higher for the monomeric complex, $[Ru(CO)_2(P^nBu_3)_2(-C\equiv C-C_6H_5)_2]$ (**3**), by 39 cm^{-1} than for $[Ru(DEPE)_2(-C\equiv C-C_6H_5)_2]$ [7], a complex containing only phosphine ligands on Ru;

(iii) similarly, the $\nu_{C\equiv C}$-stretching frequency for the polymeric complexes, $[-Ru(CO)_2(P^nBu_3)_2-C\equiv C-R-C\equiv C-]_n$ (**8**, **9**) is about 39 cm^{-1} higher than for the analogous complexes conaining only the phosphine ligands, $[-Ru(DEPE)_2-C\equiv C-R-C\equiv C-]_n$;

(iv) a comparison of the IR spectra of $[Ru(PMe_3)_4(-C\equiv C-C_6H_5)_2]$ (2055 cm^{-1}) [5b], $[Ru(DEPE)_2(-C\equiv C-C_6H_5)_2]$ (2054 cm^{-1}) [7], and $[Pt(PEt_3)_2(-C\equiv C-C_6H_5)_2]$ (2100 cm^{-1}) [10] indicates that the $\nu_{C\equiv C}$-stretching frequency is lowered by approximately 45 cm^{-1} when a Group 10 (d^8) metal is replaced by a Group 8 (d^6) metal. However, there is a small change (7 cm^{-1}) in the stretching frequency when the mixed auxiliary ligand complex $[Ru(CO)_2(P^nBu_3)_2(-C\equiv C-C_6H_5)_2]$ (**3**) (2093 cm^{-1}) and $[Pt(PEt_3)_2(-C\equiv C-C_6H_5)_2]$ are compared. These results, together with those of optical spectra presented above, demonstrate that auxiliary ligands on the metal play a vital role in determining the metal-to-alkyne ligand charge transfer. The strong π-acceptor character of the CO ligands introduces considerable back bonding to bound carbonyls in $[-Ru(CO)_2(P^nBu_3)_2$-σ-alkyne)] complexes, and hence there is less electron charge transfer to alkyne ligands than in the corresponding complexes

TABLE 1.

Compound	IR $\nu_{C\equiv C}$ (cm^{-1})	Band gap, E_g (eV)
$[Ru(CO)_2(P^nBu_3)_2(-C\equiv C-C_6H_5)_2]$ [a] (**3**)	2093	–
$[Ru(DEPE)_2(-C\equiv C-C_6H_5)_2]$ [a] [7]	2054	3.60
$[Ru(PMe_3)_4(-C\equiv C-C_6H_5)_2]$ [a] [5b]	2055	–
$[Pt(PEt_3)_2(-C\equiv C-C_6H_5)_2]$ [a] [5]	2100	–
$[ClRu(CO)_2(P^nBu_3)_2(-C\equiv C-p-C_6H_4-C_6H_4-C\equiv C-Ru(CO)_2(P^nBu_3)_2Cl]$ [a] (**5**)	2105	4.40
$[ClPt(P^nBu_3)_2-C\equiv C-p-C_6H_4-C\equiv C-Pt(P^nBu_3)_2Cl]$ [a] [9]	2114	3.60
$[-Ru(DEPE)_2-C\equiv C-p-C_6H_4-C\equiv C-]_n$ [a]	2046	3.19
$[-Ru(DEPE)_2-C\equiv C-p-C_6H_2(CH3)_2-C\equiv C-]_n$ [a]	2045	3.25
$[-Ru(DEPE)_2-C\equiv C-p-C_6H_4-C_6H_4-p-C\equiv C-]_n$ [a]	2046	3.07
$[-Ru(PMe_3)_4-C\equiv C-p-C_6H_4-C_6H_4-p-C\equiv C-]_n$ [b]	2046	–
$[-Ru(CO)_2(P^nBu_3)_2-C\equiv C-p-C_6H_4-C\equiv C-]_n$ [a] (**8**)	2084	3.51
$[-Ru(CO)_2(P^nBu_3)_2-C\equiv C-p-(CH_3)_2C_6H_2-C\equiv C-]_n$ [a] (**9**)	2085	3.50
$[-Pt(P^nBu_3)_2-C\equiv C-p-C_6H_4-C\equiv C-]_n$ [a] [9]	2095	3.26

[a] IR measured in dichloromethane. [b] IR measured in Nujol.

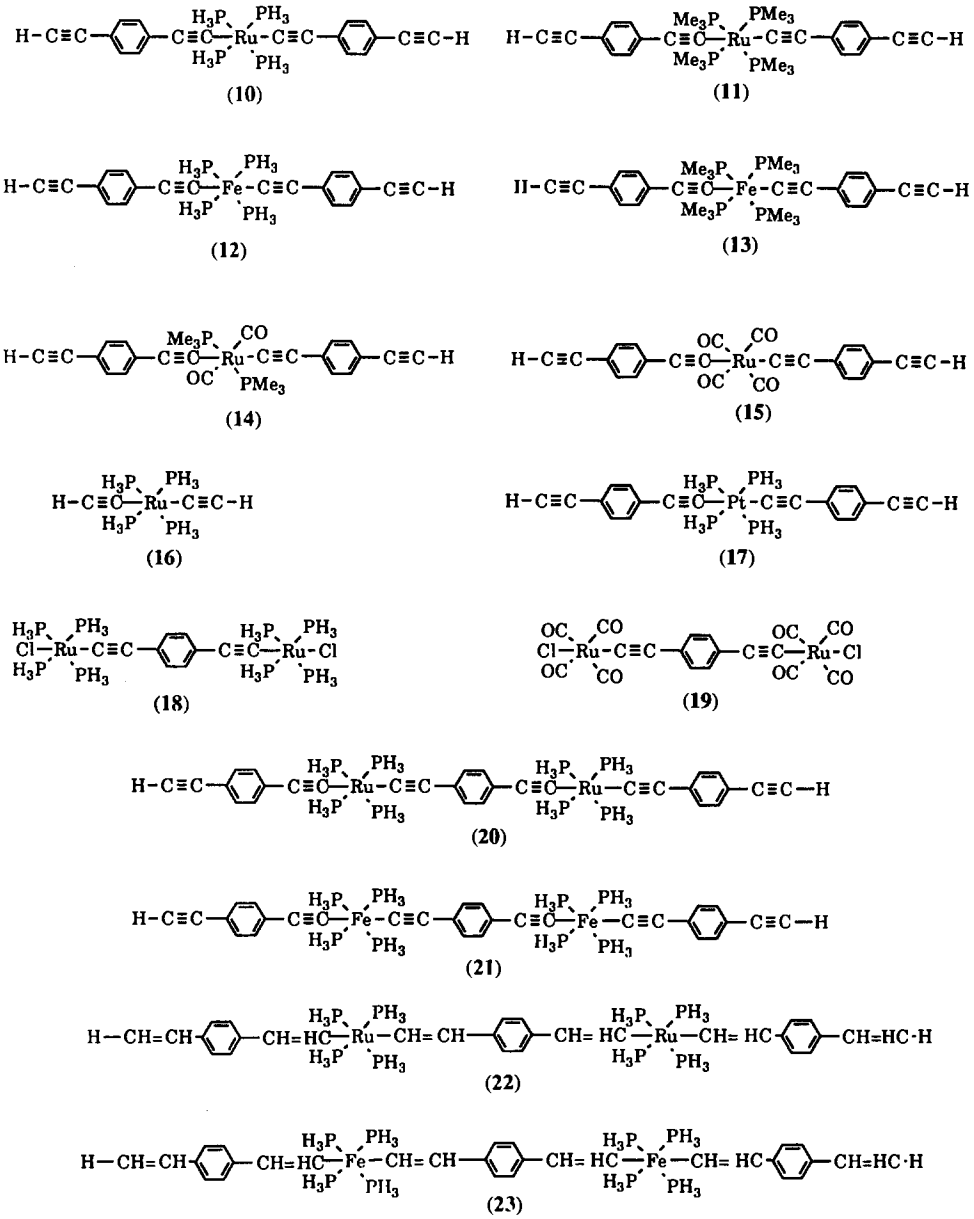

Scheme 2.

bearing strong donor auxiliary ligands on the metal. This in turn increases or decreases the extent of π-conjugation in the backbone.

2.3. Molecular orbital calculations

The results of Fenske-Hall molecular orbital calculations on the model complexes (Scheme 2, **10–23**) are presented in Table 2. For the $[ML_4](RH)_2$ (Fig. 1) and $[M(L)_4(RH)]_2R$ (L = PH_3, PMe_3; R = alkynyl, alkenyl) (Fig. 2) complexes, the molecular orbital scheme obtained is that expected for a d^6 metal ion in an approximately octahedral field, with the alkynyl or alkenyl ligands and the phosphine ligands interacting nearly equally with the metal d-orbitals. The metal d_{z^2} and $d_{x^2-y^2}$ orbitals [11*] interact with lone pair orbitals of the six ligands to form occupied σ-bonding orbitals and a high-lying unoccupied e_g-like set of orbitals. The t_{2g}-like occupied metal d_{xy}, d_{xz}, and d_{yz} orbitals do not mix substantially with the ligand orbitals. Instead, they form a set of metal-based orbitals close in energy to the d-orbitals of the metal (as indicated by the

* Reference number with an asterisk indicates a note in the list references.

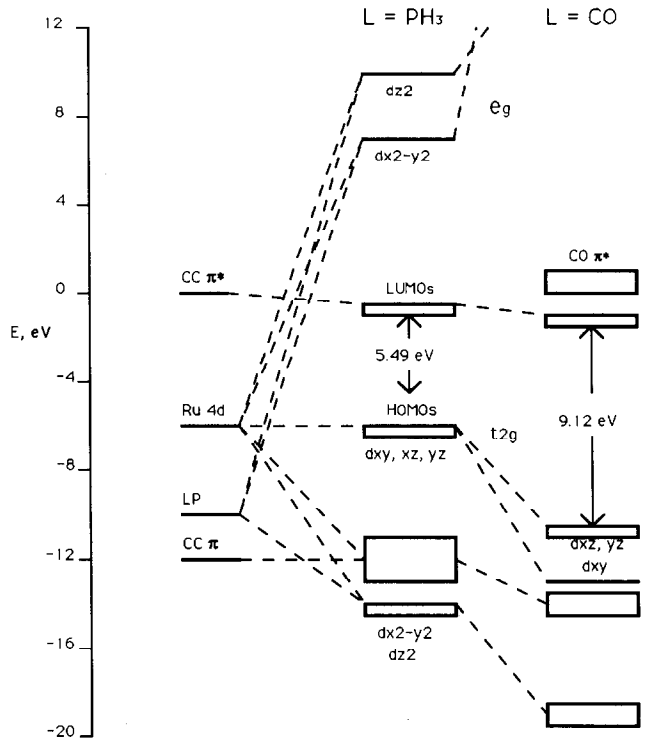

Fig. 1. Molecular orbital diagram for $[RuL_4(-C{\equiv}C-p-C_6H_4-C{\equiv}C-H)_2]$ (L = PH_3 (**10**); CO (**17**)).

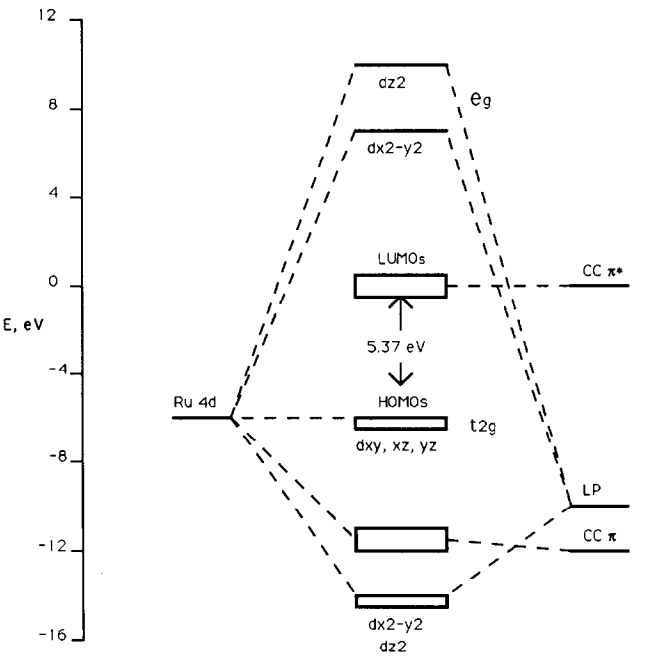

Fig. 2. Molecular orbital diagram for $[H-C{\equiv}C-p-C_6H_4-C{\equiv}C-Ru(PH_3)_4-C{\equiv}C-pC_6H_4-C{\equiv}C-Ru(PH_3)_4-C{\equiv}C-p-C_6H_4-C{\equiv}C-H]$ (**20**).

diagonal atomic d-orbital energies of the Fock matrix). The highest-energy orbital of this t_{2g}-like set (the d_{yz} or d_{xz} orbital) is therefore the highest occupied molecular orbital (HOMO) of the compound. In a similar manner, the π_y^* antibonding molecular orbitals of the alkynyl or alkenyl ligands, which do not mix significantly with the metal orbitals, are close in the energy to the π^* orbitals of the ligand fragments, and are spread

TABLE 2.

Compound	Energy (eV)		
	HOMO	LUMO	GAP
$[Ru(PH_3)_4(-C{\equiv}C-p-C_6H_4-C{\equiv}C-H)_2]$ (**10**)	−6.35	−0.86	5.49
$[Ru(PMe_3)_4(-C{\equiv}C-p-C_6H_4-C{\equiv}C-H)_2]$ (**11**)	−4.78	−0.58	4.20
$[Fe(PH_3)_4(-C{\equiv}C-p-C_6H_4-C{\equiv}C-H)_2]$ (**12**)	−5.22	−1.01	4.21
$[Fe(PMe_3)_3(-C{\equiv}C-p-C_6H_4-C{\equiv}C-H)_2]$ (**13**)	−3.50	−0.75	2.75
$[Ru(PH_3)_2(CO)_2(-C{\equiv}C-p-C_6H_4-C{\equiv}C-H0_2]$ (**14**)	−8.23	−1.15	7.08
$[Ru(CO)_4(-C{\equiv}C-p-C_6H_4-C{\equiv}C-H)_2]$ (**15**)	−10.54	−1.42	9.12
$[Ru(PH_3)_4(-C{\equiv}C-H)_2]$ (**16**)	−5.85	−7.09	12.94
(to π_y^* instead of LUMO)	–	8.99	14.84
$[Pt(PH_3)_2(-C{\equiv}C-p-C_6H_4-C{\equiv}C-H)_2]$ (**17**)	−9.70	−1.96	7.74
$[Ru(PH_3)_4Cl]_2(-C{\equiv}C-p-C_6H_4-C{\equiv}C-)]$ (**18**)	−5.43	0.64	6.07
$[Ru(CO)_4Cl]_2(-C{\equiv}C-p-C_6H_4-C{\equiv}C-)]$ (**19**)	−9.20	−1.22	7.98
$[Ru(PH_3)_4]_2(-C{\equiv}C-p-C_6H_4-C{\equiv}C-)(-C{\equiv}C-p-C_6H_4-C{\equiv}C-H)_2]^n$ (**20**)			
$n = 0$	−5.98	−0.61	5.37
$n = 1+$	−9.83 (t_{2g})	−2.65 (π_y^*)	7.18
$n = 1-$	−3.88 (t_{2g})	2.19 (π_y^*)	6.07
$[Fe(PH_3)_4]_2(-C{\equiv}C-p-C_6H_4-C{\equiv}C-)(-C{\equiv}C-p-C_6H_4-C{\equiv}C-H)_2]$ (**21**)	−4.93	−0.85	4.08
$[Ru(PH_3)_4]_2(-CH{=}CH-p-C_6H_4-CH{=}CH-)(-CH{=}(CH-p-C_6H_4-CH{=}CH_2)_2]$ (**22**)	−5.96	−2.46	3.50
$[Fe(PH_3)_4]_2(-CH{=}CH-p-C_6H_4-CH{=}CH-)(-CH{=}CH-p-C_6H_4-CH{=}CH_2)_2]$ (**23**)	−5.14	−2.64	2.50

relatively little in energy, with the lowest-lying of these orbitals serving as the lowest-unoccupied molecular orbital (LUMO) for the compound. The molecular orbital pattern obtained for the $M(CO)_4(RH)_2$ compounds is similar, but with the expected greater interaction of the CO π and π^* orbitals with the d-orbitals of the metal. For the $Pt(PH_3)_2(RH)_2$ compounds, the splitting pattern is that expected for an approximately square planar d^8 system, also with a metal-based HOMO and acetylenic π^* LUMO. The dominant interactions and orbital compositions obtained here with the Fenske-Hall model are in good qualitative agreement with the results of closely related extended Hückel calculations carried out by Frapper and Kertesz [12]. As found by Kostic and Fenske [13] for Cp-metal acetylide complexes, the π^* acetylide ligand orbitals do not contribute significantly to the occupied frontier orbitals for these complexes.

The predominantly metal-d-orbital character of the HOMO and ligand π^*-orbital character of the LUMO for all of these compounds provide a ready rationalization for the trends observed in Table 2. Replacing PH_3 by the better σ-donor PMe_3 should increase the electron density on the metal ion, destabilize the metal d-orbitals, and raise the energy of the HOMO (without significantly changing the energy of the predominantly ligand π^* LUMO), and thereby decrease the HOMO–LUMO gap. Comparison of the data for $[M(PH_3)_4](C{\equiv}C{-}C_6H_4{-}C{\equiv}C{-}H)_2$ (**10**, **12**) and $[M(PMe_3)_4](C{\equiv}C{-}C_6H_4{-}C{\equiv}C{-}H)_2$ (**11**, **13**) (M = Fe, Ru) shows that replacing PH_3 by PMe_3 destabilizes the t_{2g}-like HOMO by 1.6–1.7 eV, while the acetylenic π^* LUMO is destabilized by only 0.3 eV, lowering the HOMO-LUMO gap by 1.3–1.4 eV, as expected. The reverse is true, as expected, for the π-acceptor ligand CO. Replacing two of the four PH_3 ligands with CO to make $[Ru(PH_3)_2(CO)_2](C{\equiv}C{-}C_6H_4{-}C{\equiv}C{-}H)_2$ (**14**) removes electron density from the t_{2g}-like HOMO, lowering its energy by 1.9 eV (while the LUMO is stabilized by only 0.3 eV), and increasing the HOMO–LUMO gap by 1.6 eV. Replacing the two remaining PH_3 ligands by CO to form $[Ru(CO)_4](C{\equiv}C{-}C_6H_4{-}C{\equiv}C{-}H)_2$ (**15**) increases the HOMO–LUMO gap by an additional 2.0 eV. Similar trends are evident for the dichloro complexes, where replacing the four PH_3 ligands of $[ClRu(PH_3)_4{-}C{\equiv}C{-}C_6H_4{-}C{\equiv}C{-}Ru(PH_3)_4Cl]$ (**18**) by CO (**19**) ligands increases the HOMO–LUMO gap by 1.9 eV. These shifts in electron density are also reflected by the Mulliken atomic charge on the metal, which changes from −0.69 e for ruthenium in $[Ru(PH_3)_4](C{\equiv}C{-}C_6H_4{-}C{\equiv}C{-}H)_2$ to −0.24 e for ruthenium in $[Ru(PH_3)_2(CO)_2](C{\equiv}C{-}C_6H_4{-}C{\equiv}C{-}H)_2$, and to +0.03 e for the ruthenium in $[Ru(CO)_4](C{\equiv}C{-}C_6H_4{-}C{\equiv}C{-}H)_2$.

The effects of oxidation and reduction on the frontier orbitals are shown by examining the series $(H{-}C{\equiv}C{-}C_6H_4{-}C{\equiv}C{-}Ru(PH_3)_4{-}C{\equiv}C{-}C_6H_4{-}C{\equiv}C{-}Ru(PH_3)_4{-}C{\equiv}C{-}C_6H_4{-}C{\equiv}C{-}H)^n$ (**20**) with $n = 0, \pm 1$. Oxidizing the neutral compound to its monocation removes an electron from the t_{2g}-like HOMO, stabilizing it by 3.8 eV, while the ligand-based LUMO is stabilized by only 2.0 eV, giving rise to an increase of 1.8 eV in the HOMO–LUMO gap. Reducing the neutral compound to its monoanion adds an electron to the ligand-based π^* LUMO, destabilizing it by 2.8 eV while the metal-based HOMO is destabilized by only 2.1 eV, increasing the HOMO–LUMO gap by 0.7 eV. Thus, both removing an electron from the metal-based HOMO and adding an electron to the ligand-based LUMO lead to an increase in the HOMO–LUMO gap.

Changing the metal also alters the HOMO–LUMO gap, as seen from the results for $[ML_4](C{\equiv}C{-}C_6H_4{-}C{\equiv}C{-}H)_2$ (L = PH_3; PMe_3; M = Fe (**12**, **13**), Ru (**10**, **11**). Replacing ruthenium with iron has little effect on the ligand-based LUMO (stabilizing it by only 0.2 eV), but a significantly larger effect on the metal-based HOMO, destabilizing the latter by 1.1–1.3 eV to lower the HOMO–LUMO gap by 1.3–1.4 eV. This change largely reflects the relative energies of the metal d-orbitals, with the diagonal term of the Fock matrix for the iron 3d orbitals lying 1.3–1.4 eV above that for the ruthenium 4d orbitals in this set of compounds. A corresponding comparison for the bimetallic alkyne and alkene compounds $[M(PH_3)_4]_2(C{\equiv}C{-}C_6H_4{-}C{\equiv}C{-}H)_2(C{\equiv}C{-}C_6H_4{-}C{\equiv}C{-})$ (**20**, **21**) and $[M(PH_3)_4]_2(CH{=}CH{-}C_6H_4{-}CH{=}CH{-}H)_2(CH{=}CH{-}C_6H_4{-}CH{=}C{-}H)$ (**22**, **23**) reveals a similar decrease in the HOMO–LUMO gap of 0.7–1.0 eV when ruthenium is replaced with iron.

The nature of the conjugated ligand "backbone" for these polymers also plays a crucial role in the energenetics of the frontier orbitals by controlling the relative energy of the π^* LUMO. As shown by Frapper and Kertesz [12] for conjugated acetylenes of the type $\{-C{\equiv}C-\}_n$, initial coupling of acetylenes produces a large decrease in the energy of the acetylenic π^*-antibonding orbitals, and a somewhat smaller increase in the energy of acetylenic π-bonding orbitals to reduce the HOMO–LUMO gap greatly, but the additional stabilization gained with added acetylenic units becomes quite small after $n = 4$ or 5. Similarly, we find a large decrease in the energy of the acetylenic π^* orbitals on going from $[Ru(PH_3)_4](C{\equiv}C{-}H)_2$ (**16**) at +8.99 eV to $[Ru(PH_3)_4](C{\equiv}C{-}C_6H_4{-}C{\equiv}C{-}H)_2$ (**10**) at −0.86 eV with a corresponding large decrease in the HOMO–LUMO gap, but further ligand conjugation is likely to provide only marginal decreases in the ligand

π^* energy and consequently in the HOMO–LUMO gap. It is tempting to view the decrease in the HOMO–LUMO gap with an increasing number of acetylenic units in the compound (from 6.07 eV for $[Ru(PH_3)_4]_2(C{\equiv}C{-}C_6H_4{-}C{\equiv}C{-})Cl_2$ (**18**) with one conjugated ligand to 5.49 eV for $[Ru(PH_3)_4](C{\equiv}C{-}C_6H_4{-}C{\equiv}C{-}H)_2$ (**10**) with two, and finally to 5.37 eV for $[Ru(PH_3)_4](C{\equiv}C{-}C_6H_4{-}C{\equiv}C{-}H)_2(C{\equiv}C{-}C_6H_4{-}C{\equiv}C{-})$ (**20**) with three) as a reflection of conjugation throughout the compound and, by implication, an expected further decrease in band gap upon polymerization. However, the rather small drop (0.1 eV) in the HOMO–LUMO gap upon going from two ligands to three suggests that conjugation between adjacent ligands through the linking metal ion is small, as would be expected since the LUMO and other slightly higher energy π^* orbitals have very little metal character. From these calculations it appears that although the "valence band" for these polymers may contain significant mixing of the metal d-orbitals and the ligand π-orbitals as judged from the composition of the HOMO and orbitals immediately below in energy), the "conduction band" will be composed primarily of ligand π^* orbitals that will be delocalized within each individual ligand but not significantly delocalized between ligands across the metal centers. For a more complete picture of these effects, see the band structure calculations of Frapper and Kertesz [12].

A change of hybridization for the conjugated ligand, however, may be more promising as a means of reducing the HOMO–LUMO gap. Changing from acetylenic (with a C≡C triple bond at 1.20 Å) to ethylenic groups (with a C=C double bond at 1.40 Å) in the ligand should lower the energy of the ligand-based π^* LUMO by decreasing the overlap of the $2p\pi$ carbon orbitals, and by providing a better energy match between the π-orbitals of the sp^2-hybridized ethylene (as opposed to sp-hybridized acetylene) and the π-orbitals of the sp^2-hybridized phenyl ring. That this is indeed the case can be seen by comparing $[M(PH_3)_4]_2(-C{\equiv}C{-}C_6H_4{-}C{\equiv}C{-}H)_2(-C{\equiv}C{-}C_6H_4{-}C{\equiv}C{-})$ (**20**, **21**) and $[M(PH_3)_4]_2(-CH{=}CH{-}C_6H_4{-}CH{=}CH{-}H)_2(-CH{=}CH{-}C_6H_4{-}CH{=}C{-}H{-})$ (**22**, **23**) (M = Ru, Fe). Replacing the acetylenic ligand by an ethylenic ligand lowers the energy of the ligand-based π^* LUMO significantly (1.8 eV) while the metal-based t_{2g}-like HOMO is less affected (stabilized by only 0.0–0.2 eV), significantly lowering the HOMO–LUMO gap by 1.6–1.9 eV.

3. Summary

The particular transition metal, auxiliary ligands, and the bridging alkyne units play a significant role in determining the degree of π-electron delocalization in rigid rod transition metal σ-acetylide complexes. The fact that these effects appear to be roughly separable and additive gives support to arguments from chemical intuition and experience, and act as guides for designing new systems for synthesis and evaluation. Although calculations on these smaller idealized molecular model systems should not be expected to be in quantitative agreement with band gaps observed experimentally for polymeric materials, the HOMO–LUMO gap of 4.20 eV predicted for $[Ru(PMe_3)_4](C{\equiv}C{-}C_6H_4{-}C{\equiv}C{-}H)_2$ with its more realistic trialkylphosphine ligands, is encouragingly near the band gaps of 3.1–3.2 eV observed experimentally here for the $Ru(DEPE)_2$-based polymers.

4. Experimental details

All reactions (unless otherwise specified) were carried out under nitrogen by glove box or Schlenk line techniques. Solvents were dried and distilled from appropriate drying agents. Infrared spectra were recorded on a Perkin-Elmer 1710 Fourier Transform Spectrometer. Optical absorption measurements were carried out using a Q-switched Nd:YAG laser operating at 266 nm. The spectra were recorded for dilute solutions in dichloromethane. $Me_3Sn{-}C{\equiv}C{-}C_6H_5$ (**2**) was prepared from phenylacetylene, and the bis-Me_3Sn-alkyne reagents (**4**,**6**,**7**) were prepared by modification and adaptation of literature procedures [10]. Synthesis of the complexes $M(DEPE)_2(-C{\equiv}C{-}C_6H_5)_2$ and $[-M(DEPE)_2(-C{\equiv}C{-}R{-}C{\equiv}C{-}]_n$ (M = Fe, Ru; DEPE = 1,2-bis(diethylphosphino)ethane; R = p-C_6H_4, p-$(CH_3)_2)C_6H_2$) has been reported previously [7].

Molecular orbital calculations were carried out using the Fenske-Hall Model [14]. For the molecular structures, idealized from the results of the X-ray crystal structural study of *trans*-$Ru(DPPE)_2(C{\equiv}C{-}C_6H_5)_2$, [7] the bond lengths used were M–P, 2.36 Å, M–C≡C, 2.06 Å, M–CH–C, 2.06 Å, M–CO, 1.916 Å, M–Cl, 2.39 Å, P–H, 1.42 Å, P–C, 1.84 Å, C–O, 1.125 Å, C_{sp}–C_{sp}, 1.20 Å, C_{sp}–C_{sp^2}, 1.46 Å, C_{sp^2}–C_{sp^2}, 1.40 Å, C_{sp}–H, 1.06 Å, C_{sp^2}–H, 1.10 Å and C_{sp^3}–H, 1.10 Å. Bond angles were 180° for C_{sp}, 120° for C_{sp^2}, and 99° for PH_3 and PMe_3. The DPPE ligands were modeled as PH_3 or PMe_3, and an all-*trans* configuration for the alkene ligand was used. Basis functions [15] for ground state atomic configurations were used, except for transition metals, which assumed $d^{n+1}s^0$ cationic configurations with exponents of 2.00 (Fe), 2.20 (Ru), and 2.40 (Pt) for the outermost s and p orbitals. Calculations were carried out initially for each ligand separately, then for each molecule transformed from the ligand fragments with low-lying occupied σ-bonding and the correspond-

ing unoccupied virtual σ-antibonding orbitals frozen out of the calculation as ligand core orbitals [16].

4.1. Synthesis

4.1.1. $Ru(CO)_2(P^nBu_3)_2(C{\equiv}C{-}C_6H_5)_2$ (3)

To a solution of $Me_3Sn{-}C{\equiv}C{-}C_6H_5$ (**2**) (0.120 g, 0.25 mmol) in 60 mL of tetrahydrofuran (THF) were added 0.063 g (0.1 mmol) of $Ru(CO)_2(P^nBu_3)_2Cl_2$ (**1**) and 5 mg of CuI. The mixture was stirred at 40°C for about 14 h and THF was then removed *in vacuo*. The residue was purified by column chromatography on neutral grade 1 alumina with dichloromethane as eluant. Compound (**3**) was obtained as a very pale yellow solid in 80% yield.

Anal. Found: C, 65.89; H, 8.48. $C_{42}H_{64}O_2P_2Ru$ calc.: C, 66.02; H, 8.44%. Mass spectrum (+FAB m/z) of parent ion: found 764; calc. 764.3. (IR, CH_2Cl_2) ν_{CO} 1987 cm^{-1}, $\nu_{C{\equiv}C}$ 2093 cm^{-1}.

4.1.2. $Cl(CO)_2(P^nBu_3)_2Ru{-}C{\equiv}C{-}p{-}C_6H_4{-}C_6H_4{-}C{\equiv}Ru(P^nBu_3)_2(CO)_2Cl$ (5)

To a solution of $Ru(CO)_2(P^nBu_3)_2Cl_2$ (**1**) (0.190 g, 0.3 mmol) in 50 mL THF was added 0.078 g (0.15 mmol) of $Me_3Sn{-}C{\equiv}C{-}C_6H_4{-}C_6H_4{-}C{\equiv}C{-}SnMe_3$ (**4**), and the mixture was stirred at 35–40°C for 24 h, the THF was then removed *in vacuo*, and the residue purified on an alumina column with dichloromethane as eluant. The solid residue obtained after evaporation of dichloromethane *in vacuo* was washed several times with dry methanol to give compound (**5**) as a yellow solid in 84% yield.

Anal. Found: C, 58.51; H, 8.30. $C_{68}H_{116}O_4P_4Cl_2Ru_2$ calc.: C, 58.56; H, 8.38%. (+FAB, m/z) of parent ion: found 1395; calc. 1394.5 (IR, CH_2Cl_2) ν_{CO} 1989 cm^{-1}, $\nu_{C{\equiv}C}$ 2106 cm^{-1}.

4.1.3. $[-(CO)_2(P^nBu_3)_2Ru{-}C{\equiv}C{-}R{-}C{\equiv}C{-}]_n$ (R = $p{-}C_6H_4$ (8), $p{-}C_6H_2(CH_3)_2$ (9))

The polymeric complexes (**8**,**9**) were prepared by the general procedure outlined here for $[-(CO)_2(P^nBu_3)_2Ru{-}C{\equiv}C{-}C_6H_4{-}C{\equiv}C{-}]_n$. A solution of $Ru(CO)_2(P^nBu_3)_2Cl_2$ (**1**) (0.126 g, 0.2 mmol), $Me_3Sn{-}C{\equiv}C{-}C_6H_4{-}C{\equiv}C{-}SnMe_3$ (**6**) (0.09 g, 0.2 mmol) and 10 mg of CuI in 50 mL of dichloromethane was stirred at 40°C for 24 h. The solution was cooled to room temperature and eluted through an alumina column with dichloromethane. The volume of dichloromethane eluate was reduced by half *in vacuo* and methanol was added to precipitate the product. The crude solid was washed with methanol several times and dried *in vacuo* to yield the polymer as a yellow solid in 81% yield.

Anal. Found: C, 62.91; H, 8.57. $C_{36}H_{58}O_2P_2Ru$ calc: C, 63.04; H, 8.52%. M_W = 58064 (n_W = 80). (IR, CH_2Cl_2) ν_{CC} 1988 cm^{-1}, $\nu_{C{\equiv}C}$ 2084 cm^{-1}.

4.1.4. $[-(CO)_2(P^nBu_3)_2Ru{-}C{\equiv}C{-}C_6H_2(CH_3)_2{-}C{\equiv}C{-}]_n$ (9)

Anal. Found: C, 63.78; H, 8.62. $C_{38}H_{62}P_2O_2Ru$ calc.: C, 63.93; H, 8.75%. M_W = 59568 (n_W = 83). (IR, CH_2Cl_2) ν_{CO} 1989 cm^{-1}, $\nu_{C{\equiv}C}$ 2085 cm^{-1}.

Acknowledgments

We thank the SERC (M.S. Khan, S.L. Ingham), Kobe Steel Europe Ltd. (M.S. Khan) and the NSERC of Canada (A.K. Kakkar) for financial support. We also thank Dr. I. Hinton at Ciba-Geigy Plastics for determination of molecular weights.

References

1 J.L. Bredas and R.R. Chance, (eds.) *Conjugated Polymer Materials: Opportunities in Electronic, Optoelectronics and Molecular Electronics*, NATO ASI Series, Vol. 182, Kluwer Acad. Publ., Dordrecht, 1990.

2 Such polymers for Ni, Pd and Pt were first reported by S. Takahashi, H. Morimoto, E. Murata, S. Kataoka, K. Sonogashira and N. Hagihara, *J. Polym. Sci., Chem. Ed., 20* (1982) 565.

3 (a) A.P. Davey, D.J. Cardin, H.J. Byrne and W.J. Blau, in J. Messier,. Kajzar, P. Prasad and D. Ulrich (eds.), *Organic Molecules for Nonlinear Optics and Photonics*, Kluwer Acad. Publ., Dordrecht, 1991, p. 391; (b) W.J. Blau, H.J. Byrne, D.J. Cardin and A.P. Davey, *J. Mater. Chem., 1* (1991) 245; (c) S. Guha, C. C. Frazier, P.L. Porter, K. Kang and S.E. Finberg, *Opt. Lett., 14* (1989) 952; (d) C.C. Frazier, S. Guha, W.P. Chen., M.P. Cockerham, P.L. Porter, E.A. Chauchard and C.H. Lee, *Polymer, 28* (1987) 553.

4 S. Takahashi, Y. Takai, H. Morimoto and K. Sonogashira, *J. Chem. Soc., Chem. Commun.*, (1984) 3.

5 (a) M.S. Khan, S.J. Davies, A.K. Kakkar, D. Schwartz, B. Lin, B.F.G. Johnson and J. Lewis, *J. Organomet. Chem., 424* (1992) 87; (b) S.J. Davies, B.F.G. Johnson, J. Lewis and P.R. Raithby, *J. Organomet. Chem., 414* (1991) C51; (c) B.F.G. Johnson, A.K. Kakkar, M.S. Khan and J. Lewis, *J. Organomet. Chem., 409* (1991) C12; (d) S.J. Davies, B.F.G. Johnson, M.S. Khan and J. Lewis, *J. Chem. Soc., Chem. Commun.*, (1991) 187.

6 (a) Y. Sun, N.J. Taylor and A.J. Carty, *Organometallics, 11* (1992) 4293; (b) Y. Sun, N.J. Taylor and A.J. Carty, *J. Organomet. Chem., 423* (1992) C43.

7 Z. Atherton, C.W. Faulkner, S.L. Ingham, A.K. Kakkar, M. S. Khan, J. Lewis, N.J. Long and P.R. Raithby, *J. Organomet. Chem., 462*, (1993) 265.

8 For GPC procedural details see: S. Takahashi, M. Kariya, T. Yatake, K. Sonogashira and C.U. Pittman Jr. (eds.), *Organometallic polymers*, Academic Press, New York, 1978

9 (a) J. Lewis, M.S. Khan, A.K. Kakkar, B.F.G. Johnson, T.B. Marder, H.B. Fyfe, F. Wittmann, R.H. Friend and A.E. Dray, *J. Organomet. Chem., 425* (1992) 165; (b) B.F.G. Johnson, A.K. Kakkar, M.S. Khan, J. Lewis, A.E. Dray, F. Wittmann and R.H. Friend, *J. Mater. Chem., 1* (1991) 485; (c) A.E. Dray, F. Wittmann, R.H. Friend, A.M. Donald, M.S. Khan, J. Lewis and B.F.G. Johnson, *Synth. Met., 41–43* (1991) 871.

10 J.F. Almeida and A. Pidcock *J. Organomet. Chem.*, *209* (1981) 415.
11 The coordinate system used places the phosphine (or carbonyl) ligands in the *xy*-plane so that the metal d_{z^2} orbital points at the terminal carbon atom of a coordinated *trans*-alkyne (or alkene) ligand, with the π-electron system of the ligand phenyl ring lying in the *yz*-plane. Thus, the acetylenic (or ethylenic) π-orbitals conjugated with the π-orbitals of the ligand phenyl ring are designated π_y (bonding) or π_y^* (antibonding). For the Pt compound, the *z*-axis remains as before, the two phosphine ligands lie along the *x*-axis, and the π-electron system lies in the *yz*-plane.
12 G. Frapper and M. Kertesz, *Inorg. Chem.*, *32* (1993) 732.
13 N.M. Kostic and R.F. Fenske, *Organometallics*, *1* (1982) 974.
14 (a) M.B. Hall and R.F. Fenske, *Inorg. Chem.*, *11* (1972) 768; (b) R.F. Fenske, *Prog. Inorg. Chem.*, *21* (1976) 179; (c) R.F. Fenske, *Pure Appl. Chem.*, *27* (1971) 61.
15 Z. Lin and M.B. Hall, *Inorg. Chem.*, *30* (1991) 3817.
16 R.F. Fenske, *Pure Appl. Chem.*, *60* (1988) 1153.